

A Photographic Study of Neutrons from $\text{Al} + \text{H}^{2*}$

R. A. PECK, JR.

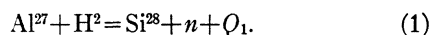
Brown University, Providence, Rhode Island

(Received May 19, 1949)

The (dn) reaction on aluminum has been studied using Eastman NTB emulsions. Twenty-two hundred head-on recoil tracks are plotted, and ten groups identified (with widths and intensities), extending up to 9 Mev excitation of the product Si^{28} nucleus. The first two excited levels, at 1.8 and 4.5 Mev, agree with gamma-ray energies and inelastic scattering. The reaction Q value (9.08 ± 0.20 Mev) determines the mass difference $\text{Si}^{28} - \text{Al}^{27} = +0.996\ 05 \pm 0.20 \times 10^{-3}$ mass unit.

EXPERIMENTAL

THE reaction studied is



Deuterons were accelerated in the Yale cyclotron, to energy 3.68 ± 0.05 Mev (mean).¹ The target was an aluminum foil of thickness 1.5 mg cm^{-2} placed perpendicular to the direction of the incident beam. After passing through the target, the deuterons were stopped in a thick backing of pure tin. (Tin was used to minimize neutrons from the backing. No exposures were made with backing only, but the Coulomb barrier height is about 2.8 Mev for aluminum, 6.8 Mev for tin.) Bombardment took place in a thick-walled brass chamber,¹ and the photographic plates were exposed immediately outside.

The plates were held (up to six at a time) in brass containers with $\frac{1}{8}$ -in. walls. The emulsions lay approximately in the target plane, so that neutrons emitted at 90° to the incident beam were recorded. The nearest end of each plate was about 6 cm from the target area (intersection of beam with target foil, about 1 cm^2 in extent), so that the detector half-angle ranged between 0.08 radian and 0.19 radian over the whole area of each plate. An exposure of about 20 micro-ampere minutes was found to give a suitable balance of neutron recoil yield and gamma-ray fog. This figure refers to the beam current as read via the tin backing on which the thin aluminum target was mounted.

Two Eastman NTB emulsions were used, Nos. 361281 and 361399, of thickness 21 and 113 microns respectively. Development was for 10 minutes in D-19 after soaking for 10 minutes in water at 30°C , and followed by fixation in F-5. Even with agitation and replenishing of the F-5, fixation times of several hours were required. After washing for 30 minutes or more the plates were dried by evaporation, lying emulsion up on absorbent paper, under an inverted dish. When completely dry the emulsions were covered with No. 0 cover glasses, using as adhesive a resin suspension (damar) in xylene.

A two-point calibration of emulsion 361281 was

* The major part of this work was done at Sloane Physics Laboratory, Yale University, New Haven, Connecticut, and assisted by the ONR under Contract No. N6ori-44.

¹ A. B. Martin, *Phys. Rev.* **72**, 378 (1947).

carried out by plotting tracks of long-range protons from $\text{B}^{10}(dp)\text{B}^{11}$ with two different values of basic absorption in the protons' path.² These emulsion ranges were compared with the air range of the same protons as determined with proportional counters.³ In this way, two values of emulsion stopping power (range in air/range in emulsion) were determined: 1975 ± 70 at 6.0 Mev and 1960 ± 180 at 3.6 Mev. Most of the assigned uncertainty is associated with the air range, and in view of the close agreement of the two stopping powers an assessment of about 1 percent error (1975 ± 20 above 3.6 Mev) seems more realistic. It is interesting that this agrees precisely with the corresponding value of Lattes, Fowler, and Cuer⁴ for the Ilford C2 plates.

Emulsion 361399 was calibrated by comparison with 361281. Six corresponding ranges in the $\text{Al}(dn)$ spectrum were identified from each emulsion, giving a stopping power for 361399 lower by 4 percent ± 1 percent than for 361281.

Tracks of recoil protons were observed with a binocular microscope (Bausch and Lomb, Model CT). To locate measurable tracks, the plates were scanned with 10X eyepieces and a 10X objective, using an oblique system of illumination. The concave mirror is adjusted to direct light obliquely through the substage condenser, with iris diaphragm wide open. Observation is at the periphery of the conic section of light which appears on the object slide. Such illumination provides the comfort of quasi-dark field, and illuminates only tracks moving in roughly the forward direction. Both features are highly desirable for the scanning operation.

For measurements, a 97X oil immersion objective was used, with the same eyepieces and the plane substage mirror (light field illumination). To be suitable for measurement, recoil tracks were required to lie within $\pm 10^\circ$ of the direction of neutron incidence, both in the horizontal and vertical planes. These angles were checked, respectively, by reference to the eyepiece scale and by the observed length of track which was in focus at a single setting. (A smaller angular spread was allowed in the vertical direction, because of the emulsion shrinkage on processing.) A criterion for the maximum acceptable elastic scattering along a track was based on

² R. A. Peck, Jr., *Phys. Rev.* **72**, 1121 (1947).

³ A. B. Martin, unpublished.

⁴ Lattes, Fowler, and Cuer, *Proc. Phys. Soc.* **59**, 883 (1947).

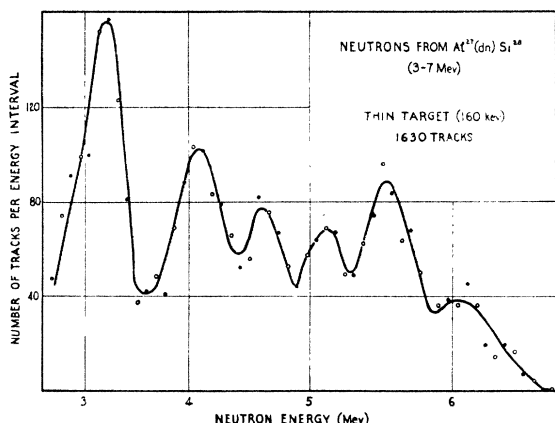


FIG. 1. Distribution of recoil energies (first part). Histogram interval=1.7 cm air equivalent in range. Each point set is a complete histogram, the two being displaced one-half interval from one another. Six groups are identified—in order of decreasing energy, III A, III B, III C, III D, III E and IV (see Tables I and II). 230 tracks (lying above 3.7 Mev) from the 113-micron thick emulsions, others from 21-micron emulsions.

the requirement that (assuming the scattering atom to be one of the lightest emulsion constituents—C, N, O) the energy lost to the recoiling atom should correspond to less than the least count of observable proton range in emulsion.

For each acceptable track, the projection on the focal plane was measured with a calibrated eyepiece scale, and the depth coordinate by the vertical travel in focussing on one end at a time (at 970X, the focal depth was about one micron). Since measured tracks lay within small angles of the horizontal plane, a sufficient correction term for the depth coordinate was the first term in the binomial expansion of $(l^2 + z^2)^{1/2}$ (l = length of projection on focal plane, z = depth difference between track ends). In view of a strong observer bias in estimating fractions of eyepiece scale divisions, all track lengths were rounded to the nearest whole scale division before further consideration. The recoil proton ranges, in the calibrated emulsions, lead to values for proton energies which, for the 0° recoils measured, are presumed to give the neutron energies directly.

The track measurements have been plotted in histogram form in Figs. 1 and 2. Against neutron energy is plotted the number of recoils observed within a fixed interval about this energy. The scale of abscissas is actually linear in range, not energy, and the collection interval is constant in range—5 scale divisions, or 1.7 cm air equivalent. In Fig. 2 this interval has been doubled because of the reduced yield at high energy. Two histograms are plotted in each of the figures, for better definition of the curve shape. The histograms are displaced from one another by a half-interval.

The distribution of observed tracks must be corrected for the energy dependence of the emulsion efficiency for neutron recording. Part of this effect is simply geometrical, due to a greater tendency for long tracks to

pass out of the emulsion, and part derives from the energy dependence of the neutron-proton scattering cross section. Both effects are calculable,⁵ and were combined in a single range-dependent correction factor applied to each ordinate in the histograms (this correction factor varied over the energy spectrum by a factor 50 for the 21-micron emulsions, a factor 6 for the 113-micron emulsions). Finally the ordinate scales were “normalized”—multiplied by the factor necessary to restore the area of each histogram (total number of tracks) to the number actually observed. Consequently the ordinates of Figs. 1 and 2 are corrected for efficiency change, but still represent correctly the over-all number of tracks observed.

EVALUATION OF GROUPS

In Figs. 1 and 2 ten groups have been identified, though the resolution in Fig. 1 does not allow much confidence in the precise location of the components of this part of the spectrum. For locating groups, the curves of Figs. 1 and 2 were used as shown. However in the determination of group parameters (range, width, intensity) each histogram was plotted and resolved separately. Thus two values were obtained for each parameter, and in Tables I and II the average of these values is used, with an assigned error equal to \pm the difference between the two values. Sole departure from this procedure was in connection with the end group, for which the yield was too low for an accurate curve shape. Here the mean range was determined arithmetically, and the width identified from the calculated standard deviation of the tracks comprising the group (root-mean-square deviation from the mean range). The intensity of the group was then taken as the height of a Gaussian curve of area equal to the number of tracks in the group, and the same width as that just determined. This procedure assumes symmetry of the end group about its mean. A partial justification of that assumption is the agreement of extrapolated—mean range, for this group, with the calculation of that quantity from expected straggling (see below).

Group symmetry was again assumed in the process of resolving Fig. 1 into separate group curves. Starting at the high energy end, the first half-group was reflected about the peak ordinate line and subtracted from the rest of the curve. The next high energy side thus “revealed” was treated in a similar fashion, and so to the low energy end of the curve. Since the group of lowest energy is quite well defined, it is possible to check the accuracy of this resolution into groups. The accumulated discrepancy (i.e., the area in Fig. 1 not accounted for) corresponds to 60 tracks, a few percent of the total number represented in Fig. 1.

Table I shows the result of reducing group energies to Q values for the reaction. The range corresponding

⁵ Geometrical correction: H. T. Richards, Phys. Rev. **59**, 796 (1941). Cross section vs. energy: see R. A. Peck, Jr., Phys. Rev. **73**, 947 (1948), footnote 9.

to the group peak was taken as mean range, converted to energy (via calibration and air range-energy curve⁶), and increased⁶ by $X_0^2 E/2 = 1.52 \times 10^{-2} E$ for critical angle $\pm 10^\circ$. The Q value was then calculated, using the known beam energy¹ and the formula for 90° observation.

It is possible to predict the over-all spread of these groups, to compare with the observed spreads.⁷ The contributing effects are range and angle straggling of protons in the emulsion, target thickness, $\pm 10^\circ$ spread allowed in collecting data, intrinsic inhomogeneity of deuteron beam and the finite size of histogram interval. The first three effects may be estimated following the procedures of Bethe.⁶ Independent information is available¹ respecting the beam inhomogeneity, and may be combined with the other straggling parameters by root-sum-squares addition.⁶ The effect of finite histogram interval may be measured empirically by applying histogram collection to a curve of known initial shape. The combination of these effects yields a prediction for the difference between extrapolated and mean range, for each group. Using the observed extrapolated range in each case, predicted mean ranges have been calculated and, in Table II, compared with the observed mean ranges. For each group, there is agreement within the cited experimental error.

The above calculations also provide predictions for half-width at half-value, which may be compared with those observed (Table II). Agreement is adequate (within cited errors) except for groups I, III *E* and IV, which may indicate that these three are multiple groups. Respecting the others it may be concluded that no intrinsic level width is observable in these experiments,

and that the number of groups extracted from Fig. 1 is about correct.

DISCUSSION OF RESULTS

The excited levels of Si^{28} indicated by this work are listed in Table I. The end group, $Q = 9.08 \pm 0.20$ Mev, leads to the mass difference $\text{Si}^{28} - \text{Al}^{27} = +0.99605 \pm 0.20 \times 10^{-3}$ mass unit.

A comparison value for the reaction Q is available from the chain

$$\text{Al}^{27} + \text{H}^2 = \text{Al}^{28} + \text{H}^1 + Q_2, \quad (2)$$

$$\text{Al}^{28} = \text{Si}^{28} + Q_3 \text{ (beta-decay)} \quad (3)$$

with (1). Eliminating the three nuclear masses, one has

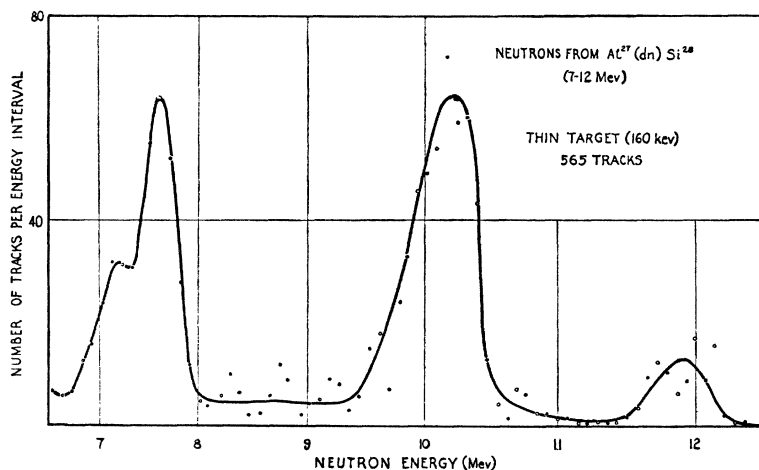
$$Q_1 = p - n + Q_2 + Q_3 = Q_2 + Q_3 - 0.80 \text{ Mev.}$$

Experimental values are $Q_2 = 5.45 \pm 0.05$ Mev⁸ and $Q_3 = 4.55 \pm 0.2$ Mev⁹ giving $Q_1 = 9.20 \pm 0.25$ Mev, in adequate agreement with the present observation. The agreement is impaired, however, by the choice of a higher Q_3 .¹⁰

The energy level scheme may be compared with gamma-ray energies from Si^{28} . When that nucleus is formed by reaction (3) the disintegration energy (maximum excitation of Si^{28}) is about 4.5 Mev and a single gamma-ray is observed, energy 1.8 Mev.⁹ This agrees well with the location of the first excited level here obtained. The absence of radiation from the second and third levels of the present scheme might indicate a Q_3 too small to excite the Si^{28} level at 4.5 Mev, or a selection rule concerning that state.

The gamma-rays from $\text{Al} + \text{H}^2$ were observed by

FIG. 2. Distribution of recoil energies (second part). Histogram interval = 3.4 cm air equivalent in range. Each point set is a complete histogram, the two being displaced one-half interval from one another. Four groups are identified—in order of decreasing energy 0, I, II *A* and II *B* (see Tables I and II). 365 of the tracks from 113-micron emulsions, others from 21-micron emulsions.



⁶ M. S. Livingston and H. A. Bethe, Rev. Mod. Phys. 9, 245 (1937).

⁷ These calculations follow a procedure worked out by H. T. Motz, to whom the author is indebted for helpful discussions of straggling problems. See R. F. Humphreys and H. T. Motz, Phys. Rev. 74, 1232 (1948). The arbitrary choice of a histogram interval in photographic work is tantamount to arbitrary "peaking" of proportional counters.

⁸ Pollard, Sailor, and Wyly, Phys. Rev. 75, 725 (1949).

⁹ W. H. Barkas, Phys. Rev. 72, 346 (1947).

¹⁰ Footnote 8 of reference 9. Also Benes, Hedgran and Hole, Arkiv. 35A, 12 (1948); Dunworth, Nature 159, 436 (1947). These papers suggest that Q_3 is 0.25 Mev higher than the value compared in the text.

TABLE I. Groups in the neutron spectrum. All energies in Mev. Reliability refers to certainty or uncertainty of existence of some group, not to group location. Errors listed are exclusive of that in stopping power, which introduces an additional ± 0.07 Mev in the end group Q value.

Group	Reliability	Relative intensity	Mean energy	Q	Si^{28} excitation
0	+	1.0 ± 0.1	12.09 ± 0.08	9.08 ± 0.13	0.00
I	+	4.4 ± 0.9	10.37 ± 0.05	7.30 ± 0.10	1.78 ± 0.13
II A	+	4.0 ± 0.2	7.75 ± 0.02	4.61 ± 0.07	4.47 ± 0.10
II B	-	2.1 ± 0.1	7.32 ± 0.13	4.17 ± 0.18	4.91 ± 0.21
III A	+	5.4 ± 0.8	6.16 ± 0.02	2.97 ± 0.07	6.11 ± 0.10
III B	+	12.0 ± 1.6	5.65 ± 0.06	2.43 ± 0.11	6.65 ± 0.14
III C	-	9.4 ± 0.1	5.21 ± 0.04	1.98 ± 0.09	7.10 ± 0.12
III D	-	10.6 ± 1.0	4.77 ± 0.04	1.53 ± 0.09	7.55 ± 0.12
III E	+	13.8 ± 0.2	4.17 ± 0.02	0.90 ± 0.04	8.18 ± 0.10
IV	+	20.6 ± 0.6	3.23 ± 0.09	-0.08 ± 0.14	9.16 ± 0.17

Alburger,¹¹ who found the same low energy gamma (1.72 ± 0.08 Mev), and others at 8.5 ± 0.5 Mev and possibly 3.0 ± 0.2 Mev. The 8.5 Mev radiation is consistent with a transition from level III E, or even IV, to ground. The 3 Mev would fit a transition to the first excited level from either of the pair II A, B (or a combination), in which connection it may be recalled that the beta-transition from Al^{28} is also to the first excited state (1.8 Mev), not directly to ground.⁹ It is possible, of course, that Alburger's gammas do not derive from the (dn) reaction.

Si^{28} gamma-radiation has also been studied by Plain *et al.*,¹² as a result of proton bombardment of aluminum. At proton energies corresponding to excitation in Si^{28} of 11.1, 11.2, 11.6 and 12.0 Mev they found average gamma-energy (respectively) 6.1, 6.5, 7.7 and 8.2 Mev. If the excitation levels found in the present work are weighted by the observed group intensities and averaged, the value 7.0 Mev is obtained; if the highest group (9 Mev) is omitted, the average falls to 6.3 Mev.

A direct check on the second excited level here reported is provided by the inelastic scattering studies of Fulbright and Bush,¹³ who assign to Si^{28} a level at 4.6 ± 0.3 Mev.

According to the statistical theory of Weisskopf¹⁴ the spectrum is expected to have a Maxwellian form

$$W_n(E) \propto E \exp(-E/T)$$

(on which the group structure already discussed is superimposed). The left-hand member represents the number of neutrons emitted (per unit energy interval)

¹¹ D. E. Alburger, Phys. Rev. **75**, 51 (1949).

¹² Plain, Herb, Hudson, and Warren, Phys. Rev. **57**, 187 (1940).

¹³ H. W. Fulbright and R. R. Bush, Phys. Rev. **74**, 1323 (1948).

¹⁴ V. F. Weisskopf, Phys. Rev. **52**, 295 (1937).

TABLE II. Group widths. First column is predicted from observed extrapolated ranges and straggling calculations. Unit is eyepiece scale division = 0.34 cm air equivalent. Last column lists half-widths calculated due to straggling only (histogram interval approaching zero). Comparison with column 5 shows the effect of finite histogram interval.

Group	Mean range in scale div.		Half-width at half maximum value (in cm air equivalent)		
	Predicted	Observed	Observed	Calculated	Differential
0	464	465 ± 6	5.0	4.8	2.8
I	355 ± 9	354 ± 3	5.7 ± 2.0	4.1	2.4
II A	213 ± 4	211 ± 1	3.7 ± 0.8	3.2	1.8
II B	187 ± 4	191 ± 6	3.5 ± 1.3	3.0	1.7
III A	144 ± 7	142 ± 1	2.7 ± 0.1	2.6	1.5
III B	121 ± 1	121 ± 2	2.6 ± 0.7	2.4	1.4
III C	104 ± 1	105 ± 2	2.4 ± 0.2	2.3	1.3
III D	88 ± 1	90 ± 2	2.0 ± 0.5	2.1	1.2
III E	75 ± 2	72 ± 1	2.6 ± 0.2	1.9	1.1
IV	49 ± 1	46 ± 2	2.4 ± 0.3	1.6	0.9

with energy E . T is the nuclear temperature (in energy units) corresponding to the maximum excitation energy of the product nucleus $\text{Si}^{28}(E_A - E_0)$, in the notation of Weisskopf). The latter is

$$\begin{aligned} E_A - E_0 &= \text{Al}^{27} + \text{H}^2 + \text{beam energy} - \text{Si}^{28} - n^1 \\ &= \text{maximum } Q \text{ value} + \text{beam energy} \\ &= 9.08 + 3.68 = 12.76 \text{ Mev.} \end{aligned}$$

Hence, if the data are plotted in the form $\ln(W/E)$ vs. E , a straight line is expected whose slope is negative and equal to the reciprocal of the nuclear temperature at excitation 12.8 Mev.

When the present data are so plotted there remains considerable scattering of points. The best visually fitted straight line has a slope

$$\frac{d[\ln(W/E)]}{dE} = -0.69 \pm 0.16 \text{ Mev}^{-1}$$

from which $T = 1.5 \pm 0.4$ Mev at 12.8 Mev excitation. We may also estimate the proportionality constant a ¹⁴ (representative of the low lying level spacing),

$$a = T^2/E = 0.19 \pm 0.09 \text{ Mev.}$$

This is in line with the estimates of Weisskopf (0.1–0.2 Mev) but is an order of magnitude smaller than the spacing of the low lying levels in Si^{28} here observed.

The Maxwell distribution corresponding to the above temperature has mean energy 3.0 Mev, its peak at $E = T = 1.5$ Mev, and falls to $1/e$ of maximum at $E = 0.2$ and 4.8 Mev. The data do not extend to sufficiently low neutron energies to permit observation of the peak of this Maxwell curve.